PHYSICAL REVIEW D VOLUME 21, NUMBER 10 15 MAY 1980

Gravitational wave perturbations and gauge conditions

Joan Centrella
Institute of Astronomy, Madingley Road, Cambridge CB3 0HA, England
*and Center for Relativity, University of Texas, Austin, Texas 78712**
(Received 22 October 1979)

We numerically evolve initial data modeling gravitational wave perturbations about a background Kasner cosmology. We examine the gravitational waves present in the initial data, and show that these inhomogeneities on the initial slice are not merely gauge effects. The evolution of these gravitational waves is gauge dependent, but we are able to separate the effects of the gauge terms from the true decay rate of the perturbations.

I. INTRODUCTION

Perturbation calculations have been the subject of great interest and much work in general relativity and cosmology for many years. Mathematically, perturbation techniques have been used to solve the field equations in the hope of gaining insight into the nature of general solutions by considering small deviations from highly symmetric spacetimes.[1] Astrophysical interest in primordial black-hole formation[2] and in the gravitational instability theory of galaxy formation[3]—both of which are based on the growth of small fluctuations from a spatially homogeneous spacetime—has spurred much work with perturbations. The numerical methods[4] developed over the past decade for solving the Einstein equations will yield many exciting developments for relativity as a whole and cosmology in particular, since they allow us to construct inhomogeneous spacetimes having strong gravitational fields and realistic matter sources. In this paper we will study the evolution of perturbations within this modern context of numerical relativity.

In the case of matter-filled cosmologies, we know that the density contrast of a perturbation with wavelength larger than the horizon size will grow until the horizon exceeds the wavelength.[5] Afterwards, restoring forces due to the pressure terms will cause the amplitude of the perturbation to oscillate. Studies of gravitational wave perturbations in anisotropic cosmologies[6] show that similar effects arise even in the absence of matter: The perturbations are oscillatory once they fall within the horizon, with the curvature providing the restoring forces. We are thus led to consider initial data that look like perturbations of a background Kasner model, hoping that the evolution of these vacuum data will provide a good basis for further calculations in more realistic models.

Before beginning our analysis in earnest, we wish to make a few remarks regarding gauge problems in general relativity. Einstein has provided us with a beautiful and satisfying theory which gives the physical laws in a gauge-invariant form, but when we perform calculations using the field equations, we are forced to choose a specific coordinate system. These calculations are plagued by seemingly "physical" effects which are, in fact, merely the manifestations of a bad choice of coordinates. Clearly, the evolution of galaxies or primordial black holes will have physical meaning only if it is possible to separate the gauge terms from the true growth rate. In this work we will be vigilant in our search for such coordinate effects and will take care to elucidate their contribution to the evolution of perturbations.

II. INITIAL DATA FOR VACUUM PERTURBATIONS

Numerical relativists solve the field equations by considering general relativity from the point of view of its Cauchy problem. Within this framework our first task in evolving perturbations of vacuum cosmologies is thus to set up an appropriate initial slice by specifying values for the three-metric γ_{ij} and the extrinsic curvature $K^i{}_j$ that satisfy the constraint equations. Centrella and Matzner[7] have shown how to set initial data that resemble a different Kasner model at each value z on an initial hypersurface. We will adopt their method in setting up our initial slice.

We therefore write the Kasner metric in the form

$$ds^2 = -dt^2 + (t/t_0)^{2p_1}dx^2 + (t/t_0)^{2p_2}dy^2 + (t/t_0)^{2p_3}dz^2 , \tag{2.1}$$

where t_0 and p_i are constants, and

$$p_1 + p_2 + p_3 = 1 , \tag{2.2a}$$

$$p_1^2 + p_2^2 + p_3^2 = 1 . \tag{2.2b}$$

To set the initial data we choose

$$\gamma_{ij}=\delta_{ij}$$

and generalize t_0 and the anisotropy parameters p_i to be functions of z. We are free to specify this function $t_0(z)$, which gives the age of the Kasner model at each value of z at the match epoch. Choosing

$$t_0(z)=A\sin(kz)+B\,, \tag{2.3}$$

we then have a set of Kasner models with smoothly varying ages. The momentum constraint gives the condition

$$p_3(z)=Vt_0(z)+1=VA\sin(kz)+(VB+1)\,, \tag{2.4}$$

where the constant $V<0$ can be chosen freely. From this relation we see that these universes also have smoothly varying anisotropy parameters. We thus interpret these initial data as perturbations around a background Kasner universe with age and anisotropy parameter given by

$$t_{\rm 0bkgnd}=\langle t_0(z)\rangle=B\,, \tag{2.5a}$$

$$p_{\rm 3bkgnd}=\langle p_3(z)\rangle=VB+1\,, \tag{2.5b}$$

where $\langle\ \rangle$ denotes an average over z.

Notice that this choice of data does not lead to simple sinusoidal perturbations in $K^i{}_j$ on the initial slice. For instance,

$$K^z{}_z=-\frac{p_3(z)}{t_0(z)}=-\frac{VA\sin(kz)+(VB+1)}{A\sin(kz)+B}\,, \tag{2.6}$$

which clearly shows that nonlinear terms appear in $K^z{}_z$. The other components of the extrinsic curvature are even more complicated, with terms such as $\sin^2(kz)$ appearing in the numerator. We will make the assumption later that the wave number k dominates the dynamics, but we should keep in mind that these initial data are more complex than the monochromatic plane waves used in the linearized treatment of perturbations. However, these data do satisfy the constraint equations exactly (i.e., to the round-off error in the computer), in contrast to the analytic results which only satisfy the field equations to first order in the perturbation amplitude.

Before proceeding further with our analysis of vacuum perturbations, we will pause to ask the following question: Are the inhomogeneities we have introduced merely gauge effects, brought about by our choice of coordinate system? Our perturbation initial data consist of Kasner models that vary smoothly around the background universe, and we need to ask whether this inhomogeneous slice is in fact simply a distorted slice through a Kasner model. If it is, data which are explicitly of Kasner models can be evolved to the inhomogeneous slice in a small time interval δt using a general lapse function and shift vector. In Appendix A we show that it is not, in general, possible to carry out this procedure, so we can be assured that our initial data really represent a slice from a spatially inhomogeneous cosmology.

III. GRAVITATIONAL WAVES IN THE INITIAL DATA

We will now look more closely at our initial data set to gain a better understanding of the physical scenario it represents. As it stands, the initial data

$$\gamma_{ij}=\delta_{ij}\,, \tag{3.1a}$$

$$K^i{}_j=K^i{}_j(z)\ \text{ diagonal} \tag{3.1b}$$

tell us only that our intrinsically flat initial slice is curved in the full four-dimensional spacetime. Physically, there is gravitational-wave energy in the extrinsic curvature which bends the slice; the waves carrying this energy will manifest themselves in the three-metric as the data are evolved. There are, however, many difficulties inherent in defining gravitational waves in general spacetimes, as discussed at great length in the literature.[8] Followng the general consensus, we will take the point of view that the gravitational wave modes lie in the transverse-tracless (TT) parts of the metric.

To get an idea of the gravitational waves stored on the initial surface, we will look at the gravitational wave modes in the time derivative of the three-metric at the initial time. The trick used to solve the initial-value constraint equations, $\gamma_{ij}=\delta_{ij}$, led us to put the perturbations on the initial slice into the extrinsic curvature. However, this condition also leads to a description of the gravitational waves induced in γ_{ij} by these perturbations in terms of the linearized theory of gravity.

We shall use the evolution equations for γ_{ij} in the form given in Appendix A. Using a zero-shift vector and a lapse $\alpha=1$ in Eq. (A4), we have

$$\partial_t\gamma_{ij}=-2K_{ij}\,.$$

Expanding the time derivative in a Taylor series and keeping only first-order terms, we see that

$$\gamma_{ij}(z,t_i+\delta t)=\delta_{ij}-2\delta tK_{ij}(z,t_i)=\delta_{ij}+h_{ij}\,, \tag{3.2}$$

where δt is a small parameter and t_i is the initial time. Since we can always arrange

$$|h_{ij}|=2\delta t\,|K_{ij}(z,t_i)|\ll 1\,,$$

the expression (3.2) for $\gamma_{ij}(z,t_i+\delta t)$ looks like that given by linearized theory, and so we will say that the gravitational waves at a time δt to the future of the initial slice are in the TT part of h_{ij}. We stress, however, that the background

spacetime is the Kasner model and not Minkowski space; in fact, the background itself has a nonzero TT time derivative.

Since we are dealing with gravitational waves of one polarization and a diagonal metric, we find that the time derivative of the transverse-traceless parts of h_{ij} are

$$\frac{\partial h^{yy}_{TT}}{\partial t} = K_{xx} - K_{yy}\,, \tag{3.3a}$$

$$\frac{\partial h^{xx}_{TT}}{\partial t} = -\frac{\partial h^{yy}_{TT}}{\partial t}\,, \tag{3.3b}$$

with all other components zero. This result may be obtained from an explicit calculation of the TT pieces of h_{ij} by using the York decomposition procedure[9] which is done in Appendix B.

For the perturbation initial data,

$$K_{xx} = -\frac{1}{3t_0}(\cos\theta + \sqrt{3}\sin\theta + 1) = -\frac{p_1}{t_0} \tag{3.4a}$$

and

$$K_{yy} = \frac{1}{3t_0}(\cos\theta - \sqrt{3}\,\sin\theta + 1) = -\frac{p_2}{t_0}\,, \tag{3.4b}$$

where $\cos\theta = -\frac{3}{2}Vt_0 - 1$. These perturbations thus induce a gravitational wave

$$\frac{\partial h^{yy}_{TT}}{\partial t} = -\frac{2}{\sqrt{3}}\frac{\sin\theta}{t_0} = \frac{p_2 - p_1}{t_0} \tag{3.5}$$

at $t = t_1$.

As a specific example, take $t_0(z)$ as given by (2.3) with $A = 0.5$ and $B = 4$. Choosing $V = -\frac{1}{6}$, we notice that the horizon size in the background cosmology defined by t_0 is

$$z_{\text{horiz}} = -1/V = 6\,. \tag{3.6}$$

For the background, then,

$$\left.\frac{\partial h^{yy}_{TT}}{\partial t}\right|_{\text{bkgnd}} = -\frac{1}{2\sqrt{3}} = -0.288\,68\,. \tag{3.7}$$

We wish to compare this result to the average of the same quantity in the perturbed spacetime:

$$\left\langle \frac{\partial h^{yy}_{TT}}{\partial t} \right\rangle = \frac{1}{2\pi}\int_0^{2\pi} \frac{\partial h^{yy}_{TT}}{\partial t}(z)\,dz$$

$$= \frac{-1}{\sqrt{3}\,\pi}\int_0^{2\pi} \frac{\sin\theta(z)}{t_0(z)}\,dz\,. \tag{3.8}$$

We evaluate the integral in (3.8) numerically, using the extended Simpson's rule on an evenly spaced mesh.[10] Considering both long-($k = 1$) and short- ($k = 10$) wavelength perturbations, we find that to the accuracy of 10^{-5}, they yield the same average value for h^{yy}_{TT},

$$\left\langle \frac{\partial h^{yy}_{TT}}{\partial t} \right\rangle = -0.289\,81\,. \tag{3.9}$$

Notice, however, that this number is larger in magnitude than the background value (3.7); i.e., the waves contribute a direct-current (DC) piece by themselves. Since a single monochromatic wave in the metric would average to the background value, this result is indicative of the fact that the perturbations are a superposition of such modes. We attribute this DC piece to the homogeneous, $k = 0$ mode perturbation, which corresponds to changing the background Kasner universe[11] (i.e., changing the values of the p_i).

IV. REVIEW OF ANALYTIC PERTURBATION STUDIES

We will now look at the numerical evolution of the initial data

$$t_0 = A\sin(kz) + B$$

set up in Sec. II. Since we are using the computer to build a spacetime that is "unknown" in the sense that there is no analytic expression for the metric $g_{\mu\nu}$ to compare with our computed values, we look to other perturbation studies to see the kinds of behavior we might encounter. The analytic treatments of perturbations in anisotropic cosmologies[6,11] deal with monochromatic plane waves in the metric; as discussed in Secs. II and III, our perturbations are manifestly more complicated than this, but we shall assume that the wave number k dominates the dynamics in order to compare our results with the single-mode behavior derived analytically.

As a prelude to confronting our calculations with those derived using linearized perturbation equations, we will briefly review the analytic results, following for the most part the notation of Perko, Matzner, and Shepley.[6] The perturbed metric takes the form

$$ds^2 = -dt^2 + \sigma_{il}(\delta^l{}_j + d^l{}_j)\,dx^i\,dx^j\,, \tag{4.1}$$

where σ_{ij} is the diagonal three-metric for Bianchi type-I cosmologies. For our purposes we will further require $d^i{}_j$ to be diagonal, with $d^i{}_j = d^i{}_j(z,t)$ only. Writing the wave vector $\vec{k} = (0,0,k)$, we perform a Fourier decomposition of the metric perturbations to write

$$d^i{}_j(z,t) = \mu^i{}_j(t)e^{ikz}\,. \tag{4.2}$$

Next, we focus attention on the quantities

$$\mu = \mathrm{tr}\,\mu^i{}_j = \mu^i{}_i\,, \tag{4.3}$$

$$\eta = \tfrac{1}{2}(\mu^1{}_1 - \mu^2{}_2)\,. \tag{4.4}$$

The function μ is mainly of interest in the study of galaxy formation in dust-filled Bianchi type-I universes, since Perko *et al.* have shown that in this case it is possible to choose a gauge in which the density contrast $\Delta \equiv \delta w/w$ (where w is the en-

ergy density of the matter) satisfies

$$\Delta = -\tfrac{1}{2}\mu + \text{constant}. \tag{4.5}$$

For the case of gravitational-wave perturbations in the axisymmetric vacuum Kasner model $\vec{p} = (\frac{2}{3}, \frac{2}{3}, -\frac{1}{3})$, Hu[11] has shown that

$$\mu(t) = c_1 t^{-1} - c_2 t^{5/3}, \tag{4.6}$$

where c_1 and c_2 are constants. We thus expect our calculations to show μ growing as we evolve forward in time.

A physically more interesting quantity is η, which is a gravitational wave mode coupled to μ. As such, η is the TT part of the metric perturbation and satisfies a wave equation; in the case of dust, it is also coupled to the density contrast Δ. Studies[6] have shown that η will oscillate as long as $kH \gg 1$, where H is the horizon size in the direction of propagation of the perturbation, and the amplitude of these oscillations decreases in time.

V. EVOLUTION OF THE PERTURBATIONS

We are now ready to put this perturbation initial data into a computer program[12] that will construct a four-dimensional vacuum spacetime by solving the evolution equations numerically. Since most studies of spatially homogeneous cosmologies use geodesic slicing we shall do likewise and choose

$$\text{lapse} \quad \alpha = 1, \tag{5.1}$$

$$\text{shift} \quad \beta^i = 0. \tag{5.2}$$

In addition, we impose periodic boundary conditions on the z axis; this is particularly convenient numerically, for it eliminates the possibility of any disturbance on the boundary propagating inward and affecting the evolution of the perturbations.

The computer evolution (the evolution equations are written out explicitly in Appendix A) gives the values of the metric components $\gamma_{ij}(z)$ on each time slice, which we write as

$$\gamma_{ij}(z) = \gamma_{ij\,\text{bkgnd}} + P_{ij} = \gamma_{ij\,\text{bkgnd}}(\delta^l{}_i + d^l{}_i), \tag{5.3}$$

where P_{ij} represents the perturbation. A problem arises in choosing which values to use for the background metric. As outlined above, the $k=0$ mode present in our initial data means that the background defined by the average of the waves is not the same as that given by the average Kasner age $t_{0\,\text{bkgnd}} = B$. Our computer calculations show that this situation gets worse as the evolution proceeds, with the background metric defined by the average age $t_{0\,\text{bkgnd}}$ completely separating from the computed inhomogeneous metric. Motivated by the desire to make our results look as much like the perturbation picture as possible, we take $\langle \gamma_{ij} \rangle$ as the background metric on each slice, where $\langle\ \rangle$ denotes an average over z. The generalization of $d^i{}_j$ is therefore

$$d^i{}_j = \frac{\gamma_{ij\,\text{computed}}(z) - \langle \gamma_{ij}(z) \rangle}{\langle \gamma_{ij}(z) \rangle}, \tag{5.4}$$

with no sum on i or j. We are using a diagonal metric, and will consider only diagonal perturbations so (5.4) holds for $i=j$. Thus, choosing

$$z_{\max} = \text{peak},$$

$$z_{\min} = \text{trough}$$

of a cycle of the initial perturbations, we form the quantities

$$\mu = \tfrac{1}{2}[\mu(z_{\max}) - \mu(z_{\min})], \tag{5.5}$$

$$\eta = \tfrac{1}{2}[\eta(z_{\max}) - \eta(z_{\min})] \tag{5.6}$$

on each slice to get the amplitudes for comparison with perturbation theory.

As an example, take the initial data (2.3) with $A = 0.5$, $B = 7$, $V = -\frac{1}{6}$, and $k = 10$. These values lead to a perturbation amplitude on the initial slice of

$$|K^i{}_j(z_{\max}) - K^1{}_j(z_{\min})| \sim 10^{-2}. \tag{5.7}$$

The results of the evolution to give $\mu(t)$ and $\eta(t)$ are shown in Figs. 1 and 2. We note here that $\mu(t)$ grows in time, and that $\eta(t)$ oscillates and decays.

In order to discuss the numerical errors that enter our calculations, we must keep in mind that we are interested in relative errors. For any quantity G, the relative error ϵ is given by

$$G = G_{\text{comp}}(1 \pm \epsilon),$$

where G_{comp} is the value given by the computer code. Studies[12] of the vacuum code lead us to expect relative errors ϵ of order $\Delta t / t_{0\,\text{bkgnd}}$. The relative error in the constraints, which should equal zero in these vacuum spacetimes, is com-

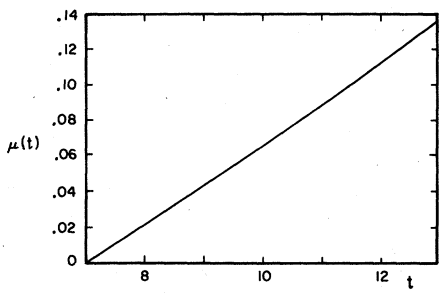

FIG. 1. In this graph μ is plotted as a function of time t. The evolution runs from $t = t_{0\,\text{bkgnd}} = 7$ to $t = 13$. For this case, $A = 0.5$, $V = -\frac{1}{6}$, and $k = 10$. Here and elsewhere, the time t is measured in arbitrary units.

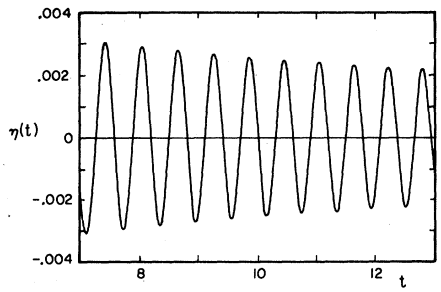

FIG. 2. This graph shows $\eta(t)$ for the same evolution and time interval as given in Fig. 1.

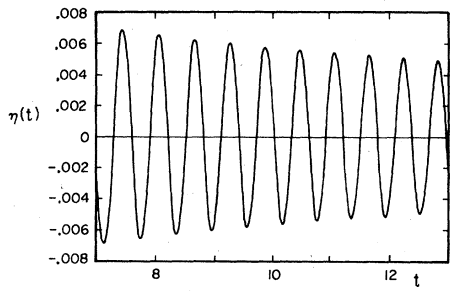

FIG. 3. This graph shows $\eta(t)$ for the same evolution and time interval as in Fig. 2 except that $A = 1.0$. In this case, the size of the perturbations on the initial slice is larger, but the number of oscillations is the same.

puted as the value of the constraints returned by the code divided by a typical magnitude of the component terms.

We have run two evolutions of these data, using first

$$\Delta t = 1.2 \times 10^{-3}$$

and then

$$\Delta t = 3.0 \times 10^{-4},$$

and the results are identical; the size of the time step does not seem to affect the evolution of these data. In both cases, the relative error in the Hamiltonian constraint is of order 10^{-5}, which is consistent with a relative error $\Delta t/t_{0\,\mathrm{bkgnd}}$ $\sim 10^{-4}$–10^{-5}. The momentum constraint held to an even higher accuracy in both evolutions. We are therefore confident that the results presented here are real and free from contamination of numerical errors.

For comparison, we ran a second set of data with $A = 1.0$, with all other parameters including t_{final}, the end point of the evolution, unchanged. These values give a perturbation size on the initial slice as defined by (5.7) as $\sim 8 \times 10^{-2}$. Two evolutions of these data were performed as above, with essentially identical results and a relative error in the constraints of 10^{-4} at worst. The results for $\eta(t)$ are shown in Fig. 3. Comparing the two cases, we find that although $|\eta|$ is larger for $A = 1$, the number of oscillations of η is the same in both instances. Apparently, the additional energy content of this wave did not affect the background enough to significantly change the wave evolution.

VI. DISCUSSION AND CONCLUSIONS

When we try to compare our results more closely with perturbation theory, we discover that there are problems due to the fact that η is *not* a gauge-invariant quantity. Our kinematical choice of lapse $\alpha = 1$ and shift $\beta^i = 0$ corresponds to the usual conditions

$$\delta g_{0\mu} = 0 \tag{6.1}$$

used in perturbation theory; however, there are four more gauge transformations consistent with (6.1). As outlined by Perko *et al.*,[6] these are the infinitesimal coordinate transformations

$$x^\mu \to \bar{x}^\mu = x^\mu + \xi^\mu , \tag{6.2}$$

$$\delta g_{\mu\nu} \to \delta \bar{g}_{\mu\nu} = \delta g_{\mu\nu} - \xi_{\mu;\nu} - \xi_{\nu;\mu} , \tag{6.3}$$

where a semicolon denotes the four-dimensional covariant derivative in the unperturbed metric. The ξ^μ consistent with (6.1) are

$$\xi^0 = -f_0(x^i) , \tag{6.4}$$

$$\xi^i = -f_{0,p} \int e^{-2\alpha} e^{-2\beta\, ip} dt + f^i(x^i) , \tag{6.5}$$

where we have written the unperturbed Kasner metric in the form

$$ds^2 = -dt^2 + e^{2\alpha} e^{2\beta\, ij}\, dx^i\, dx^j . \tag{6.6}$$

We note that the f^i correspond to a recoordinatization of one particular fixed $\tau =$ constant hypersurface, e.g., the initial slice, while f_0 corresponds to an arbitrary reshaping of this $\tau =$ constant slice. The Fourier-analyzed forms of f_0 and f^i are

$$f_0(x^i) = F_0 e^{i\vec{k}\cdot\vec{x}}, \tag{6.7}$$

$$f^i(x^i) = F^i e^{i\vec{k}\cdot\vec{x}}, \tag{6.8}$$

where F_0 and F^i are constants; they produce changes in η described by

$$\eta \to \bar{\eta} + c e^{-3\alpha} F_0 , \tag{6.9}$$

where c is a constant depending on the anisotropy parameters.

Looking at our initial data as perturbations around a background Kasner cosmology, we have found that this background is not unambiguously defined. If we choose a specific background and then look at the initial data as perturbations around it, we find that the perturbations are not

monochromatic waves as in Perko's analysis but rather more complicated functions. Thinking in terms of reshaping Perko's initial surface to look like ours, we see that we need to introduce the function f_0 defined in (6.7) above, and thus we have a gauge term coupled to η. This term decays like

$$e^{-3\alpha} = t_0/t \tag{6.10}$$

for a background Kasner model written in the form (2.1).

Furthermore, our technique of choosing initial data means that "perturbations" of different amplitudes have differing amounts of the gauge terms corresponding to f_0 and f^i. This is because our initial surface differs, by terms of the same order as the perturbations, from the τ = constant slices on which perturbations are usually imposed. Our system is definitely within the perturbation scheme when the initial data are close to a Kasner model; for gauge-dependent quantities such as η and μ, however, the gauge terms intervene to prevent comparison between our scheme and the usual perturbation formalism.

The result of these effects is that we are left not knowing how much of the decay we see in our computer evolutions of η is due to the gauge term and how much is due to real damping of the gravitational waves. All hope is not lost, however, since Perko's[6] analysis includes a treatment of a "free" gravitational wave η_f, which comes from off-diagonal metric perturbations

$$\eta_f = \mu^1{}_2$$

and represents the other polarization state for gravitational waves. Important facts to realize about η_f are that it is not coupled to the dust source terms nor is it coupled to other perturbation modes such as $\mu^1{}_1$; it is also gauge independent once we have imposed the condition (6.1).

Perko has shown that this free wave oscillates and decays once its wavelength is smaller than the horizon size, in the same manner as η. For the oscillatory regime, we may write[13]

$$\eta_f \propto J_m(kH),$$

where J_m is the Bessel function of order m and m is a constant that depends on the anisotropy of the model. Using the asymptotic form as $KH \to \infty$, we find

$$\eta_f \sim \frac{1}{\sqrt{H}} \times (\text{oscillatory terms}),$$

so that the envelope of η_f falls off as

$$\eta_{f\,\text{env}} \sim \left[\frac{t_0^{p_3}}{1-p_3} t^{1-p_3}\right]^{-1/2},$$

or

$$\eta_{f\,\text{env}} \sim \left[\frac{t_0}{1-p_3} e^{3\alpha(1-p_3)}\right]^{-1/2},$$

which is always decaying since $-\frac{1}{3} \leq p_3 < 1$. Note that $p_3 = 1$ corresponds to flat space and is excluded,[7] and that the gauge term $e^{-3\alpha}$ falls off more rapidly than the time-dependent term $(e^{3\alpha})^{-(1-p_3)/2}$ in the envelope of the free wave.

For the evolution shown in Fig. 2, we find, using (2.5b),

$$p_{3\,\text{bkgnd}} = -\tfrac{1}{6}$$

on the initial slice. Thus, the free wave decays like $t^{-7/12}$ in this background cosmology. Figure 4 shows this decay plotted on top of the actual wave evolution, where we have chosen the normalization so that the curve passes through the first peak of the oscillation. Also shown is a curve proportional to $e^{-3\alpha}$, normalized in the same fashion. Our wave η decays like the free wave initially from the starting time t_0, and so the decay seen in the computer evolution gives the actual physical behavior. The constants multiplying the gauge-dependent term in (6.9) must be small.

To further elucidate the nature of the gauge transformation that gets us from Perko's perturbed initial slice to ours, we would have to consider the transformation laws for the perturbations $\delta g_{\mu\nu}$ and $\delta K_{\mu\nu}$, where K_{Mu} is the four-dimensional extrinsic curvature tensor.[4,14] The fact that ξ^0 (and hence f_0) corresponds to a reshaping of a τ = constant hypersurface tells us that we need to consider the effects of the gauge transformation (6.2) not only on the metric but also on the extrinsic properties of the slice, due to its embedding in a four-dimensional spacetime. Such a "3+1" formulation of the perturbed Einstein equations has not yet been carried out.

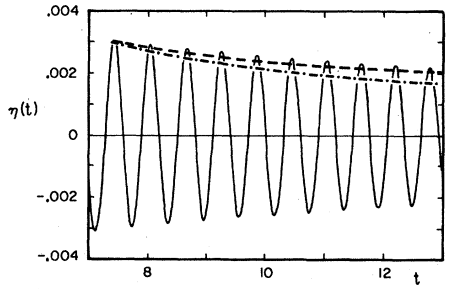

FIG. 4. This graph is the same as Fig. 2, with the decay curves for the gauge term and the free wave plotted in addition to $\eta(t)$. The dashed line marks a curve proportional to the envelope of the free wave n_f, while the dotted and dashed line shows a curve proportional to the decay of the gauge-dependent term $e^{-3\alpha}$. Note that $\eta(t)$ falls off like the free wave, which tells us that the effect of the gauge term in $\eta(t)$ is small.

This gauge problem with η serves to highlight the difficulties encountered in trying to compare analytical and computational results: The gauges and initial data convenient for one approach can easily lead to complications in the other. For example, since Perko's perturbed three-metric, by design, only satisfies the constraint equations to first order in the perturbation size, we could not have used it as initial data for the vacuum code since the smaller we make the perturbation to decrease this error, the more difficult it is to "see" the perturbation admidst the numerical errors. The finite-difference truncation error in the evolution equations would only worsen matters, and make the constraints wholly unsatisfactory on later slices. We do recognize the importance of comparing our results with analytic calculations as a touchstone as we venture forth into unknown spacetimes. We also feel, however, that it is even more important to develop methods of treating astrophysically interesting problems such as galaxy formation within the conceptual framework of numerical relativity. The radiation gauge for general relativity proposed by Smarr and York[9] may prove to be useful in this endeavor and we are investigating its importance in cosmology. Much work remains to be done in this area.

ACKNOWLEDGMENTS

I would like to thank Bernard Jones, Larry Smarr, Richard Matzner, and Ulrich Gerlach for their encouragement and enthusiasm, and for many fruitful discussions. I am pleased to acknowledge support from a Marshall Scholarship for 1975–1978 and an Amelia Earhart Fellowship Award for 1979–1980. I would also like to thank the Center for Relativity at The University of Texas at Austin for their hospitality during the academic year 1979–1980. This research forms part of a Ph.D. thesis submitted to the Institute of Astronomy, Cambridge University, England. This work was supported by NSF Grant No. PHY 7722489.

APPENDIX A: ARE THE INHOMOGENEITIES IN THE INITIAL DATA JUST GAUGE EFFECTS?

We now outline a method of showing that it is not, in general, possible to evolve initial data which are explicitly of the Kasner model to our inhomogeneous slice in a small time interval δt using a general lapse function and shift vector. The initial surface is taken to be the slice $t=t_A$ in the Kasner model of (2.1) and (2.3), and the inhomogeneous slice at $t=t_A+\delta t$ is characterized by

$$\gamma_{ij}(t_A+\delta t)=C_i=\text{constant, diagonal} \tag{A1a}$$

and

$$K_{ij}(t_A+\delta t)=K_{ij}(z),\ \text{diagonal}. \tag{A1b}$$

Using the lapse and shift

$$\alpha=\alpha(x,y,z), \tag{A2a}$$

$$\beta^i=\beta^i(x,y,z), \tag{A2b}$$

we proceed to look for contradictions among the evolution equations to show that this distortion process cannot be carried out.

Consider the evolution equations in the form[15]

$$(\partial_t-\pounds_\beta k)\gamma_{ij}=-2\alpha K_{ij}, \tag{A3}$$

$$(\partial_t-\pounds_\beta k)K_{ij}=-2\alpha K_{mi}K_j{}^m+\alpha KK_{ij}+\alpha\,{}^{(3)}R_{ij}-\alpha_{|ij}, \tag{A4}$$

where the covariant derivative, indicated by a vertical bar, and the Ricci tensor ${}^{(3)}R_{ij}$ are calculated using the three-metric γ_{ij}. $\pounds_\beta k$ is the three-dimensional Lie derivative along β^k. Since we are interested only in infinitesimal differences, we take

$$\partial_t\gamma_{ij}\big|_{t=t_A}=\frac{\gamma_{ij}(t_A+\delta t)-\gamma_{ij}(t_A)}{\delta t} \tag{A5}$$

and drop higher-order terms. Since the three-metric is constant at $t=t_A$, ${}^{(3)}R_{ij}=0$ and $\beta^k{}_{|i}=\beta^k{}_{,i}$ on the initial slice. The evolution equations thus become

$$\frac{\gamma_{ij}(t_A+\delta t)-\gamma_{ij}(t_A)}{\delta t}=(-2\alpha K_{ij}+\gamma_{kj}\partial_i\beta^k+\gamma_{ik}\partial_j\beta^k)_{t=t_A} \tag{A6}$$

and

$$\frac{K_{ij}(t_A+\delta t)-K_{ij}(t_A)}{\delta t}=(-2\alpha K_{li}K^l{}_j+\alpha KK_{ij}-\partial_i\partial_j\alpha+\beta^k\partial_kK_{ij}+K_{kj}\partial_i\beta^k+K_{ik}\partial_j\beta^k)_{t=t_A}, \tag{A7}$$

where $\partial_i=\partial/\partial x^i$.

At this stage, we have set up the twelve evolution equations to distort a slice of a Kasner model to our inhomogeneous surface in a time δt, using an arbitrary lapse and shift. We next look for inconsistencies in this set of equations to show that this process cannot be carried through. (For details, see Ref. 12.)

After some work, exhausting all the options, we are led to the situation

$$K_{xx}\big|_{t=t_A+\delta t} = K_{xx}(z) = \text{constant}\,.$$

The set of evolution equations is thus inconsistent, and the Kasner slice cannot be deformed to the inhomogeneous slice in a time interval δt.

Another way to see that the inhomogeneous data are not pure gauge begins by considering gauge transformations that preserve the translational symmetry of the Killing vectors ∂_x and ∂_y. Then note that, for linear perturbations (6.3), the quantities

$$\partial t\left[\left(\frac{t}{t_0}\right)^{1-2P_1}\delta g_{xx}\right]-\frac{P_1}{t_0}\delta g_{tt}$$

and

$$\partial_t\left[\left(\frac{t}{t_0}\right)^{1-2P_2}\delta g_{yy}\right]-\frac{P_2}{t_0}\delta g_{tt}$$

are gauge invariants. Since these quantities are zero for the unperturbed Kasner model, but are nonvanishing for our inhomogeneous slice, the initial data cannot be pure gauge.

APPENDIX B: CALCULATION OF $h^{ij}_{\rm TT}$ USING YORK'S PROCEDURE

In this appendix we shall outline York's[16] method for finding the TT parts of a tensor h^{ij}. All the tensors and covariant derivatives to be used will be defined on a three-dimensional hypersurface with metric γ_{ij}. We say that a tensor T_{ab} is transverse if

$$\nabla_b T^{ab} = 0 \tag{B1}$$

and traceless if

$$T = T^a{}_a = \gamma_{ac}T^{ac} = 0\,, \tag{B2}$$

where $a,b = 1,2,3$.

Following York, we consider a symmetric tensor h^{ab}. Its tracefree part is

$$h^{ab}_{tf} \equiv \psi^{ab} = h^{ab} - \tfrac{1}{3}h\gamma^{ab}\,. \tag{B3}$$

Then $\psi^{ab}_{\rm TT}$ is transverse traceless if

$$\psi^{ab}_{\rm TT} = \psi^{ab} - (\mathrm{LV})^{ab}\,, \tag{B4}$$

where $(\mathrm{LV})^{ab}$ is known as the longitudinal or vector part of the tensor and satisfies the equation

$$\nabla_b(\mathrm{LV})^{ab} = \nabla_b\psi^{ab}\,. \tag{B5}$$

The longitudinal part is defined in terms of a vector V^a by the equation

$$(\mathrm{LV})^{ab} = \nabla^b V^a + \nabla^a V^b - \tfrac{2}{3}\gamma^{ab}\nabla_c V^c\,. \tag{B6}$$

Its covariant derivative is

$$\nabla_b(\mathrm{LV})^{ab} \equiv (\Delta_L V)^a = \Delta V^a + \tfrac{1}{3}\nabla^a(\nabla_b V^b) + R^a{}_b V^b\,, \tag{B7}$$

where $\Delta = \gamma^{ab}\nabla_a\nabla_b$ and $R^a{}_b$ is the Ricci tensor formed from γ_{ab}.

Consider the specific case of h^{ab} given in (3.2) with $\gamma_{ab} = \delta_{ab}$. To calculate the transverse-traceless parts of h^{ab}, begin by solving (B5) for the vector V^a:

$$\nabla_b(\mathrm{LV})^{ab} = \partial_b(\mathrm{LV})^{ab} = \partial_b\psi^{ab}\,. \tag{B8}$$

Using (B7) and the fact that $R_{ab} = 0$, we have

$$\partial_z\partial_z V^a + \tfrac{1}{3}\delta^{az}\partial_z(\partial_z V^z) = \partial_z\psi^{az}\,, \tag{B9}$$

since we are only considering functions of z. The x and y components of this equation yield, for $j = 1,2$,

$$\frac{\partial^2 V^j}{\partial z^2} = 0\,, \tag{B10}$$

while the z component gives

$$\frac{\partial^2 V^z}{\partial z^2} = \frac{3}{4}\frac{\partial\psi^{zz}}{\partial z}\,. \tag{B11}$$

Thus,

$$V^z = \tfrac{3}{4}\int\psi^{zz}\,dz + c_z z + \bar{c}_z \tag{B12}$$

and

$$V^j = c_j z + \bar{c}_j\,, \tag{B13}$$

where c_a and $\bar{c}_a$ are constants and $a = 1,2,3$. Imposing the periodic boundary conditions

$$f(z) = f(z + 2\pi) \tag{B14}$$

for any function f, we immediately see that

$$V^z = \tfrac{3}{4}\int\psi^{zz}\,dz\,, \tag{B15}$$

$$V^j = c_j\,. \tag{B16}$$

Our next step is to form $(\mathrm{LV})^{ab}$ using (B6):

$$(\mathrm{LV})^{ab} = \gamma^{az}\partial_z V^b + \gamma^{bz}\partial_z V^a - \tfrac{2}{3}\gamma^{ab}\partial_z V^z\,. \tag{B17}$$

Thus,

$$(\mathrm{LV})^{zz} = \psi^{zz}\,, \tag{B18}$$

$$(\mathrm{LV})^{jj} = -\tfrac{1}{2}\psi^{zz},\quad j = 1,2,\quad \text{no sum on } j \tag{B19}$$

and

$$(\mathrm{LV})^{ab} = 0,\quad a \neq b\,. \tag{B20}$$

We can therefore form $h^{ab}_{\rm TT}$ using (B3), (B4), and (3.2) to get

$$h^{zz}_{\rm TT} = 0\,, \tag{B21}$$

$$h^{yy}_{\rm TT} = \delta t(K_{xx} - K_{yy})\,, \tag{B22}$$

$$h^{xx}_{\rm TT} = -h^{yy}_{\rm TT}\,, \tag{B23}$$

$$h^{ab}_{\rm TT} = 0,\quad a \neq b\,. \tag{B24}$$

Notice that $h^{ab}_{\rm TT}$ has only one independent component, a reflection of the fact that we are dealing with gravitational waves having only one polarization state, i.e., one degree of freedom.

*Present address.

[1]J. M. Stewart and M. Walker, Proc. R. Soc. London A341, 49 (1974).

[2]B. J. Carr, Astrophys. J. 201, 1 (1975); J. D. Barrow and B. J. Carr, Mon. Not. R. Astron. Soc. 182, 537 (1978); B. Carter, in Proceedings of the 1979 Les Houches Summer School on Physical Cosmology (unpublished).

[3]See B. J. T. Jones, Rev. Mod. Phys. 48, 107 (1976) for a review.

[4]Larry Smarr and James W. York, Phys. Rev. D 17, 2529 (1978) and references therein.

[5]S. W. Hawking, Astrophys. J. 145, 544 (1966).

[6]T. E. Perko, University of Texas Ph. D. dissertation, 1971 (unpublished); T. E. Perko, R. A. Matzner, and L. C. Shepley, Phys. Rev. D 6, 969 (1972).

[7]Joan Centrella and Richard A. Matzner, Astrophys. J. 230, 311 (1979). We set $c=8\pi G=1$. Latin indices $i,j,\ldots=1,2,3$ and Greek indices $\mu,\nu,\ldots=0,1,2,3$.

[8]Niall O'Murchadha and James W. York, Jr., Phys. Rev. D 10, 428 (1974); Charles W. Misner, Kip S. Thorne, and John Archibald Wheeler, *Gravitation* (Freeman, San Francisco, 1973); Larry Smarr and James W. York, Jr., Phys. Rev. D 17, 1945 (1978); Ref. 1.

[9]N. O'Murchadha and J. W. York, Ref. 8. This result can also be obtained from the considerations of weak gravitational waves in L. D. Landau and E. M. Lifshitz, *The Classical Theory of Fields* (Pergamon, Oxford, 1975).

[10]*Handbook of Mathematical Functions*, edited by Milton Abramowitz and Irene A. Stegun (Dover, New York, 1965).

[11]B. L. Hu, Phys. Rev. D 18, 969 (1978).

[12]The development and testing of this code are discussed in Joan Centrella, Cambridge University Ph. D. dissertation, 1979 (unpublished).

[13]We take η_f as derived by Perko for the dust case, and choose the form $\eta_f \propto J_m(kH)$ as the one which best looks like our graph of η.

[14]U. Gerlach and U. K. Sengupta, Phys. Rev. D 20, 3009 (1979).

[15]This form of the evolution equations is commonly used in numerical work. See Ref. 4.

[16]N. O'Murchadha and J. W. York, Ref. 8.